Spherical iron oxide methyltrimethoxysilane nanocomposite for the efficient removal of lead(II) ions from wastewater: kinetic and equilibrium studies

Hamid Rashidi Nodeh[a], Marzie Shakiba[b], Mohammad Ali Gabris[c], Mehdi Esmaeili Bidhendi[d],*, Syed Shahabuddin[e],*, Rashmin Khanam[f]

[a]Department of Food, Halal and Agricultural Products, Research Center of Food Technology and Agricultural Products, Standard Research Institute (SRI), Karaj, Iran
[b]Research Center of Health and Environment, School of Health, Guilan University of Medical Sciences, Rasht, Iran
[c]Department of Chemistry, Faculty of Science, University of Tehran, Iran
[d]School of Environment, College of Engineering, University of Tehran, Tehran, Iran, email: esmaeilib@ut.ac.ir (M.E.B. Hendi)
[e]Department of Science, School of Technology, Pandit Deendayal Petroleum University, Knowledge Corridor, Raisan Village, Gandhinagar – 382007, Gujarat, India, email: syedshahab.hyd@gmail.com (S. Shahabuddin)
[f]Centre for Interdisciplinary Research in Basic Sciences, Jamia Millia Islamia, New Delhi – 110025, India

ABSTRACT

In this study, synthesis of iron oxide doped methyltrimethoxysilane (Fe_2O_3-MTMOS) spherical magnetic nanocomposite was reported, based on the simple methodology for the enhanced removal of lead ions from wastewater. The synthesized magnetic nanocomposites were comprehensively characterized by using Fourier transform infrared spectrometer, field emission scanning electron microscope, X-ray diffraction, and energy dispersive X-ray spectroscopy. Fe_2O_3-MTMOS nanocomposite was then employed as an adsorbent for lead (Pb^{2+}) and various adsorption parameters, such as pH, adsorbent dosage, contact time, and initial lead (Pb^{2+}) ions concentration were analyzed and optimized. Adsorption process has been validated with different kinetic and isotherm model, where the experimental data was found to be in good agreement with pseudo-second-order ($R^2 = 0.986$) and Freundlich isotherm ($R^2 = 0.993$) as compared with other models. The adsorption capacity of the spherical Fe_2O_3-MTMOS nanocomposite was found to be relatively higher (105.5mg g^{-1}) for lead ions. Adsorption isotherm, kinetic model, and free energy models predicted multilayer sorption pattern for lead ions onto spherical Fe_2O_3-MTMOS under physical adsorption forces.

Keywords: Methyltrimethoxysilane; Iron oxide; Lead removal; Adsorbent; Isotherm

1. Introduction

In past few decades, owing to rapid industrialization, water pollution has become one of the biggest menaces to the environment. Amongst the various potential pollutants, heavy metals possess grave danger to the ecological system, especially, to aquatic ecosystem [1]. Heavy metal ions are the substances with atomic weights ranging from 63.546 and 200.590, which are widely used in various industries [2]. Heavy metal ions, existing in elemental form or incorporated with organic species, possess significant harmful effects on human health and ecology causing serious environmental problems [3,4]. Human exposure to heavy metal ions is extremely detrimental in higher concentrations and can cause neurodegenerative disorders, liver and kidney failure, and cancer [5]. Heavy metal ions usually exists in

* Corresponding authors.

water as colloids, particulate matter, and dissolved phases [6] bestowing adverse impact on water resources and causing water pollution which is a serious global environmental problem [2]. Lead (Pb^{2+}) belongs to the class of heavy metal ions, is one of the most harmful and toxic heavy metal which is responsible for various antagonistic effects on the different tissues of humans and other living beings. Furthermore, lead ions have found to be toxic for all form of living beings and probably carcinogenic [6]. Therefore, the removal of lead ions from the aquatic environment is an important task to conserve the aquatic habitats and prevent the spread of heavy metal poisoning [2,7]. According to Environmental Protection Agency (EPA) guideline the maximum residual limit level for lead ions must be less than/equal to 0.05 mg L^{-1} in wastewater [8]. Various approaches have been applied for waste water remediation, such as adsorption, photocatalysis, membrane-based separation, electro-coagulation, biochemical, and oxidative degradation [2,9–11]. Adsorption, due to its simple operation and ease of recovery, has been used most widely used for removal of heavy metals ions from waste water by employing numerous adsorbents including biomasses, fly ash, resins, rice husk ash, silica gel, alumina, and activated carbon [12]. However, in adsorption process, the most important issue to deal with, is establishing high stability, surface area, and efficiency of the sorbent material. Adsorption is remarkably effective technique since it does not add to secondary pollutants, ease of handling, cost effective, and environmentally friendly [13,14]. In fact, adsorption is an electrochemical process that occurs due to the imbalance of superficial forces at the surface of sorbent material.

Nowadays with the fast progress in science and technology, the necessity of nanoparticles has become undeniable. Nanotechnology has become a versatile technique which has make scientists around the world, engineers, chemists, and physicians, capable of working at the molecular and cellular levels [15]. The wide applications of magnetic nanoparticles have paved the way for development of new methods for synthesis of novel adsorbents to be used in removing hazardous substances from aqueous media [16,17]. Magnetic nanoparticles displays fairly unique properties and therefore, are widely used in various applications including data storage, body imaging, and catalysis [17,18]. Due to their high surface area and ease of separation from the media, magnetic materials are promising adsorbents in waste water treatment [19]. Furthermore, magnetic nanoparticles are distinguished by their shape, controlled particle size, higher stability, and narrow size distribution [17]. Due to the nano size, magnetic nanoparticles possess super paramagnetic properties, and are able to offer great potentials in a variety of applications whether in their bare or coated form with surface coating and functional groups suitable for the specific use.

Iron oxides usually are the first choice when coming to magnetic materials since these oxides have better magnetic properties, non-toxicity, and stability as compared to other magnetic nanoparticles [19,20]. Silica based nanoparticles, which can be named silica nanoparticles or nano silicates, are of great interest in various researches due to their stability, low toxicity, facile synthetic route, large-scale availability, ability to combine, and functionalized with molecules and polymers, and various applications [21].

In the current investigation, we have reported a facile methodology for the fabrication of Fe_3O_4 nanoparticle doped methyltrimethoxysilane (Fe_2O_3-MTMOS) spherical nanocomposite with improved Pb^{2+} ions adsorption efficacies. Since, MTMOS is affordable, non-toxic, possesses enhanced sorption affinity, and form three-dimensional silica network, it seems to be rationale to prepare magnetic nanocomposite for easy removal of Pb^{2+} ions. Hence, iron oxide doped methyltrimethoxysilane (Fe_2O_3-MTMOS) spherical nanocomposite was prepared and used as sorbent material for the adsorption of lead ions from waste water. The adsorption mechanism was elucidated by employing various kinetic models, where the experimental data was found to be in good agreement with pseudo-second-order model (R^2 = 0.986). Freundlich, Langmuir, and Dubinin–Radushkevich, models were analyzed for predicting adsorption behavior of Pb^{2+} ions onto Fe_2O_3-MTMOS, whereas, free energy model was examined for adsorption mechanism. Thus, Fe_2O_3-MTMOS nanocomposite can be employed as an efficient adsorbent material for removal of Pb^{2+} ions and can help in tackling the issue of heavy metal poisoning in waste water.

2. Experimental

2.1. Reagents and chemicals

Iron(II) chloride tetrahydrate ($FeCl_2 \cdot 4H_2O$), Iron(III) chloride hexahydrate ($FeCl_3 \cdot 6H_2O$), titanium(IV) butoxide, methyl trimethoxysilane (MTMOS), lead nitrate ($Pb(NO_3)_2$), ammonia (25%), high performance liquid chromatography purity grade methanol, ethanol (97%), and hydrochloric acid (37%) were all obtained from Merck Chemicals (Darmstadt, Germany) and used as received. Lead metal stock solution (500 mg L^{-1}) was prepared by dissolving calculated amount of lead salt in deionized water and stored in refrigerator. Analytical grade chemicals and deionised water was used in the entire investigation.

2.2. Instrumentation

PerkinElmer Fourier transform infrared (FTIR) system (MA, USA) was run in transmission mode in the wavenumber range of 400–4,000 cm^{-1} for recording the FTIR spectra of the synthesised materials. The surface morphology and elemental analysis of Fe_2O_3-MTMOS was performed at 15 kV using a JEOL scanning electron microscope (SEM, Tokyo, Japan) equipped with energy dispersive X-ray spectroscopy (EDX).

2.3. Sorbent synthesis

Fe_2O_3-MTMOS was synthesized via sol gel method, briefly; 500 mg of the synthesized Fe^{2+} and Fe^{3+} ions were dispersed in water/methanol solution of ratio 830:12 mmol and sonicated for 30 min for homogenization. Thereafter, 1.5 mmol MTMOS was added under continuous stirring and followed by drop wise addition of 25 mmol ammonia (25%) under vigorous stirring for 15 min. The solution was then kept for 2 d at room temperature. Finally, the desired product (Fe_2O_3-MTMOS) was washed thoroughly using

deionized water, oven-dried for 24 h (100°C), and calcinated for 2 h at 450°C.

2.4. Adsorption methodology

Batch adsorption experiments were carried out to assess the adsorption efficiency of the proposed spherical nanomaterial for the removal of lead ions from wastewater. Some effective parameters such as solution pH (2–6.5), amount of sorbent (5–150 mg), contact time (10–210 min), and initial ions concentration of Pb^{2+} (10–200mg L^{-1}) were studied to optimise the performance of Fe_2O_3-MTMOS. After the attainment of adsorption equilibrium, an external magnet was used to remove the adsorbent-lead suspension and the concentration was measured by a flame atomic absorption spectroscopy. The two main parameters; removal percentage of lead ($R\%$) and equilibrium capacity Q_e (mg g^{-1}) were estimated according to Eqs. (1) and (2), respectively, given below:

$$R\% = \left(\frac{C_0 - C_e}{C_0}\right) \times 100 \tag{1}$$

$$Q_e = \left(\frac{V}{m}\right) \times \left(C_0 - C_e\right) \tag{2}$$

where C_0 and C_e are the concentrations of lead in mg L^{-1} before and after adsorption, m mass of sorbent in mg, and V the volume of aqueous sample solution in mL.

3. Result and discussion

3.1. Characterization

FTIR is a non-destructive, rapid method, which can save time to detect a pile of accessible functional groups and unstable sensitive molecules [22]. The FTIR spectrum of the synthesized material shown in Fig. 1a exhibited peaks at 3,400 and 1,600 cm^{-1} which may be attributed to the surface hydroxyl (OH) groups. Most notable the peaks at 580 cm^{-1} (Fe–O), 2,950 cm^{-1} (C–H bond in methyl group), the two sharp signals at 1,189 and 1,056 cm^{-1} (siloxane Si–O–Si) stretching vibrations confirmed the presence of the magnetite and silicate in the final product after sol–gel process. Finally, the peak at 810 cm^{-1} absorption band depicted the Si–C in MTMOS [7]. Thus, FTIR clearly illustrate the successful synthesis of magnetic Fe_2O_3-MTMOS.

Elemental composition and surface morphology of the nanocomposite were studied with EDX and SEM. Fig. 1b shows the EDX analysis of the magnetic Fe_2O_3-MTMOS. As evident from Fig. 1b, the expected elements C (12% w/w), O (40% w/w), Si (46% w/w), and Fe (1.48% w/w) are observed clearly and in an appropriate proportion. The presence of high amount of O and Si in the EDX spectrum indicates that the synthesized adsorbent is rich oxygen and silica containing functional groups which exhibits higher affinity toward metal ions. Figs. 1c and d represent the field emission scanning electron microscope (FESEM) micrograph for nanocomposite. As evident from the FESEM images, the Fe_2O_3-MTMOS exhibited perfect spherical
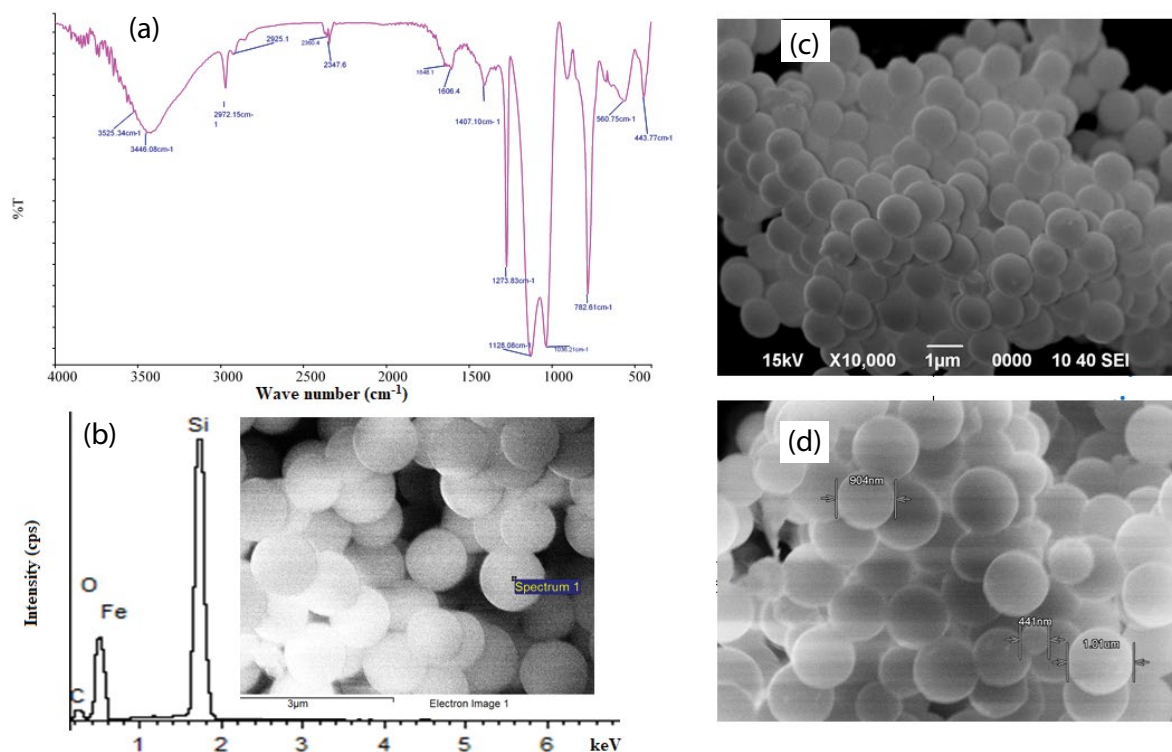

Fig. 1. (a) FTIR spectrum of Fe_2O_3-MTMOS nanocomposite, (b) EDX spectrum Fe_2O_3-MTMOS nanocomposite, (c) and (d) FESEM micrographs for spherical nanocomposite (Fe_2O_3-MTMOS).

morphology. Since the morphology of the nanocomposite is uniformly spherical, therefore, the surface area is also higher. Moreover, the magnetic nanoparticles are not visible on the surface of the nanocomposite, which signifies that the Fe_2O_3 nanoparticles are completely coated by silane groups. Thus, the morphological analysis clearly indicates the successful synthesis of spherical nanocomposites with embedded Fe_2O_3 nanoparticles within the silane matrix.

The crystalline structure of as prepared nanosphere composite was investigated with X-ray diffraction (XRD) spectroscopy as shown in Fig. 2a. The broad signal at 2θ value of 20° is an indication for MTMOS silica network. The sharp signals observed at 2θ value of 29° (220), 35° (311), 42° (400), 54° (422), 58° (334), and 63° (400) are corresponding to magnetic Fe_3O_4 nanoparticles as per the JCPDS file no. 01-071-6336. The broad signal at 20° indicates the amorphous structure for MTMOS spheres and extra sharp signals may be assigned to the cubic crystalline structure for magnetic nanoparticles.

The stability of the nanosphere composite was studied in terms of thermogravimetry analysis (TGA). Fig. 2b presents the TGA thermogram of MTMOS spheres which depicts the small weight loss (~2% w/w) and a big weight lost (~6% w/w) at 100°C–220°C and 450°C–680°C, respectively. The first weight loss may be attributed to the decomposition of hydroxyl functional groups and adsorbed free water. The second degradation may be due to decomposition of carbon based materials. Hence, the proposed material is

thermally stable material, since at temperature 100°C–700°C only 8% w/w is lost is observed.

Vibrating sample magnetometer (VSM) is an efficient technique to envisage the magnetic properties of the magnetic nanocomposites. The freshly prepared Fe_2O_3-MTMOS was studied with VSM and its magnetic hysteresis graph is shown in Fig. 2c. As can be seen in the VSM plot, the hysteresis provided an appropriate saturation magnetization (±3 emu) for Fe_2O_3-MTMOS nanosphere. Thus, this material is effectively magnetic in nature and is suitable to be removed from aqueous media by assistance of external magnetic field.

Nitrogen adsorption–desorption cycle was used to investigate the specific surface area (Brunauer–Emmett–Teller (BET)) of the magnetic nanosphere. Based on the adsorption–desorption profile (Fig. 2d), the BET surface area was found to be 20.59 m^2 g^{-1} with pore size of 0.31–1.0 nm and pore volume of 0.07 cm^2 g^{-1}. Hence, the framework structure of the as prepared Fe_2O_3-MTMOS nanosphere is mesoporous as per the IUPAC nomenclature for adsorption isotherms.

3.2. Effect of pH

Initial pH of the solution plays a vital role and is considered as one of the most important factors in sorption process, since changing of aqueous pH leads to the change in the degree of ionization and properties of both sorbent surface and metal ions [15]. The surfaces of metal oxides are usually
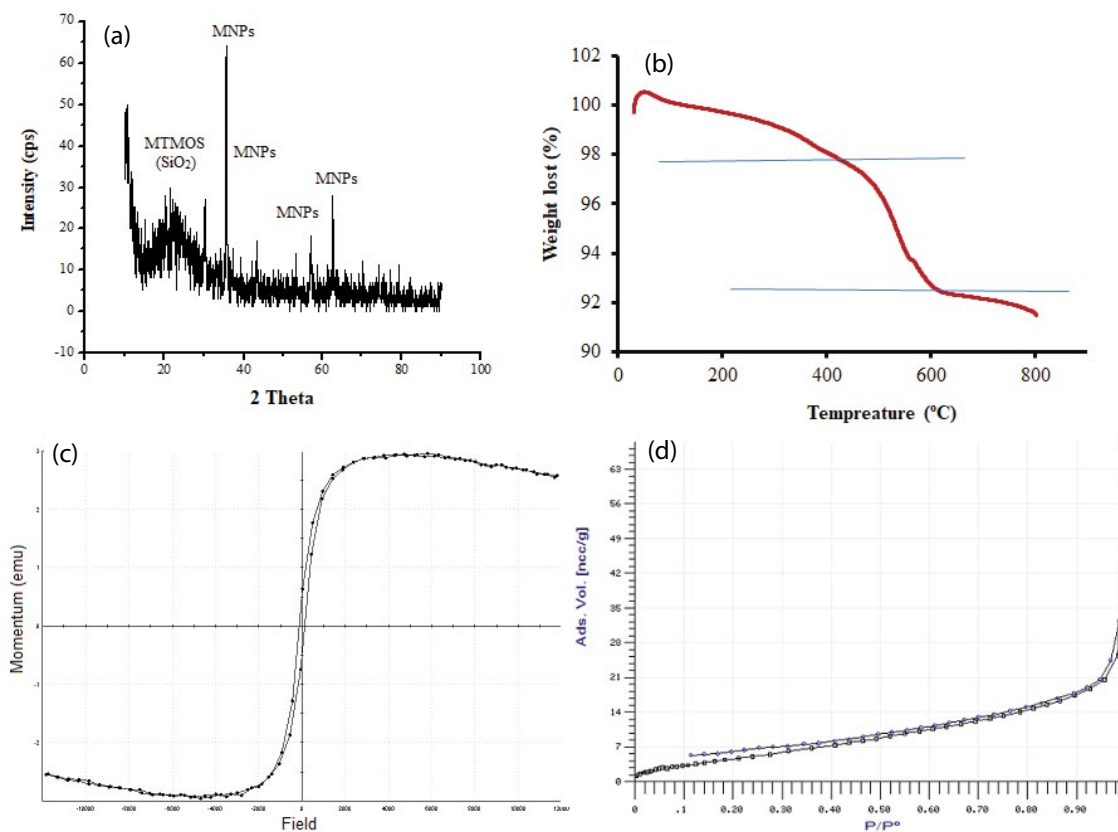

Fig. 2. (a) XRD pattern, (b) TGA graph, (c) VSM hysteresis, and (d) BET adsorption–desorption profile for Fe_2O_3-MTMOS.

comprises of hydroxyl groups that vary in form with different pH levels. In adsorption chemistry, the zero point of charge (pHzpc) is a vital parameter [23,24]. It is because, at pH < pHzpc, the adsorbent surface is positively charged and anion adsorption is more favorable and supported by electrostatic attraction while at pH > pHzpc adsorbent surface is negatively charged and cation adsorption is favorable and sustained at this point [25]. The pHzpc for magnetic-silica based materials is usually falls within the pH range of 5–6.2 [26]. Thus, in order to achieve maximum removal efficiency, effect of pH on lead removal by using Fe_2O_3-MTMOS was examined in a solution with 100 mg L^{-1} of lead ions in the pH range of 2–6.5 since at pH > 7 the lead ions under goes hydroxide precipitate [27]. As can be seen Fig. 3a, at low pH adsorption efficiency is low which may be attributed to the fact that at pH 2–4 the surface of adsorbent is positively charged (based on pHzpc) thereby causing electrostatic repulsion with metal ions. As the pH increases (from 4 to 6), the adsorption efficiency also increases since at higher pH the adsorbent surface developed negative charge leading to strong electrostatic attraction between positively charged Pb^{2+} and adsorbent.

3.3. Adsorbent dosage

The mass of sorbent is considered as another important factor affecting the adsorption efficiency of the proposed sorbent. Generally, larger doses imply greater adsorption capacity providing more active sites but just to the extent that mass transfer limitation is overcome [28]. Adsorbent dosage was examine in the range of 5–150 mg (Fig. 3b) with 100 mg L^{-1} of initial concentration of lead ions and it is clearly evident by the obtained results that by increasing the dosage the removal efficiency also increase until 80 mg. Thereafter, removal percentage remained almost constant.

3.4. Kinetic study

Adsorption rate onto Fe_3O_4-MTMS was studied by varying the contact time from 10 to 210 min as illustrated in Fig. 4a. As can be seen from the obtained results, equilibrium was accomplished after 120 min (R% > 80%) and further increase in contact time had no effect on Fe_3O_4-MTMOS adsorption capacity. It is noteworthy that the trend was steeper at the beginning and turned constant upon increasing time, implying that the removal rate was initially higher since all active sites were uncovered and available causing a stronger flux and flow of lead ions on the adsorbent. However, with time, the rate decreased significantly and reached a steady state after equilibrium due to the lesser availability of the adsorption sites and decrease in free lead concentration.

The sorption rate of lead adsorption onto Fe_3O_4-MTMOS can be described by the different kinetic models and herein pseudo-first-order and pseudo-second-order kinetic models were applied at various experimental conditions for this investigation and their corresponding linear forms were expressed respectively, as follows:
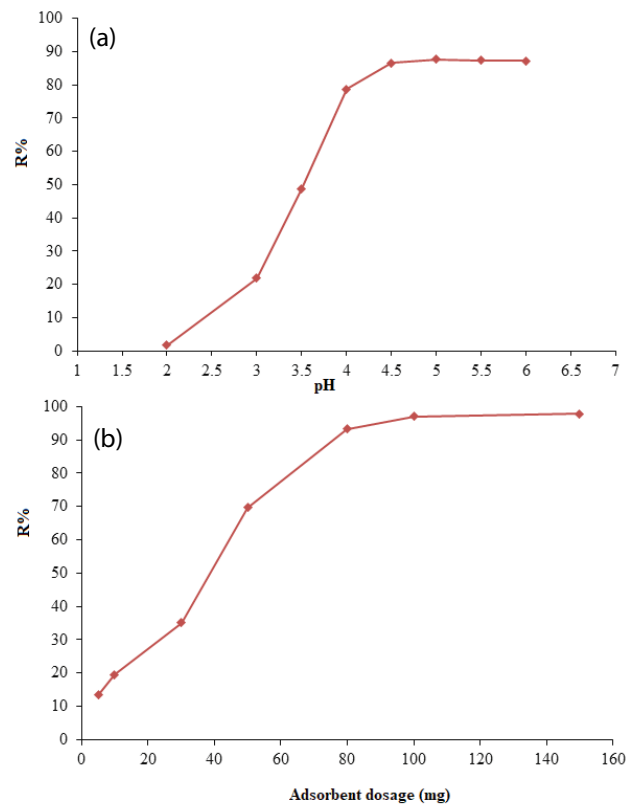
$$\ln(Q_e - Q_t) = \ln Q_e - k_1 t \tag{3}$$

Fig. 3. Effect of solution (a) pH and (b) adsorbent dosage on the adsorption process (initial concentration of lead ions 100 mg L^{-1}).

$$\frac{t}{Q_t} = \frac{1}{k_2 Q_e^2} + \frac{t}{Q_e} \tag{4}$$

where Q_e and Q_t are the adsorption capacity at equilibrium (maximum) and different time (t), respectively, in (mg g^{-1}). k_1 is the pseudo-first-order constant in (1 min^{-1}) and k_2 is the pseudo-second-order constant in (g mg^{-1} min^{-1}). The corresponding linear plots of both models are presented in Figs. 4b and c, respectively, at the same Pb^{2+} ions concentration at room temperature. The different parameters Q_e, k_1, and k_2 were estimated from the slope and y-intercept of Eqs. (5) and (6), respectively (Table 1). According to the calculated R^2 values, both models are applicable for kinetic process. In contrast, by comparing the experimental and theoretical Q_e values it was observed that pseudo-second-order fits more with the adsorption experimental data as compared to pseudo-first-order.

3.5. Isotherm study

Adsorption isotherm (Fig. 5a) is the plot of sorption capacity (Q_e, mg g^{-1}) as a function of adsorbate residual initial concentration (C_e, mg L^{-1}). These isotherms usually describe the relation between the sorbent surface coverage nature and the analytic concentration in solution at a given temperature. Besides, the prediction of adsorption mechanism at equilibrium and the optimal adsorbate amount required for the quantitative adsorption (equilibrium) can also be
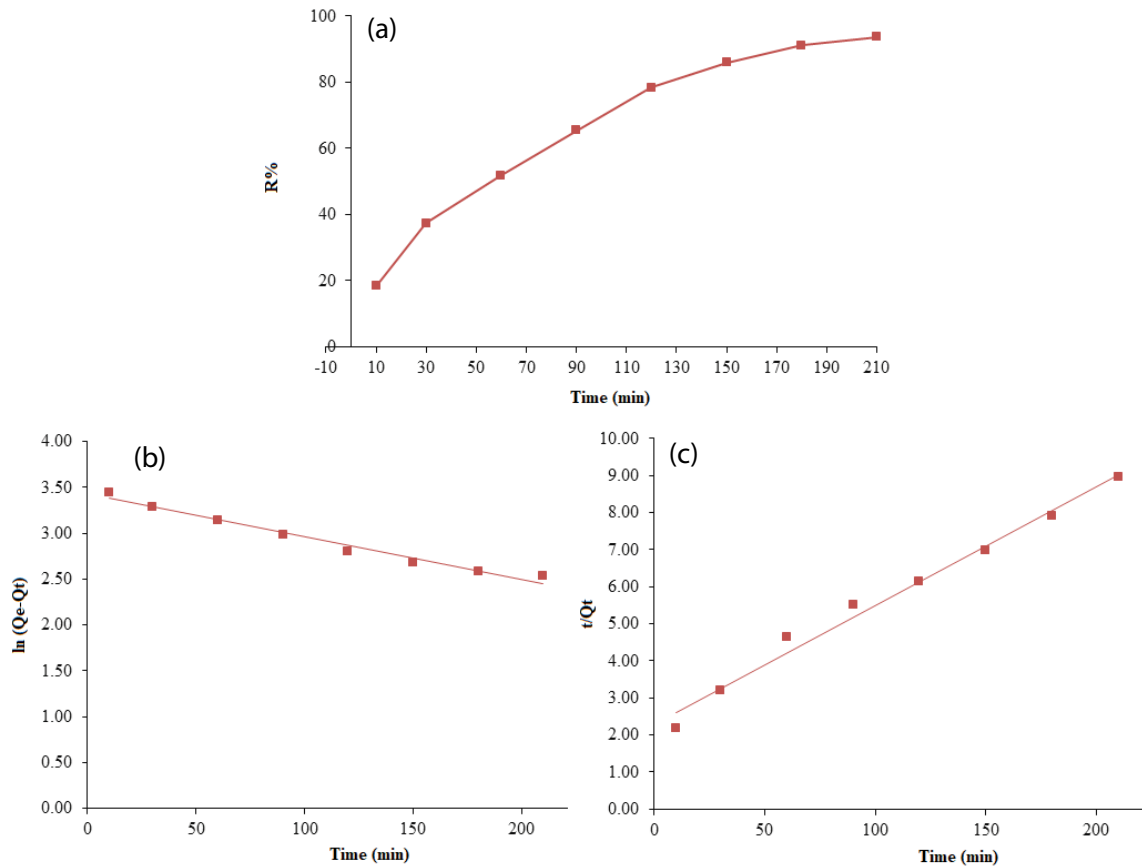
Fig. 4. (a) Effect of adsorption time on removal efficiency (initial concentration of lead ions 100 mg L^{-1}). Kinetic models of (b) pseudo-first-order and (c) pseudo-second-order.

Table 1
Kinetic models parameters for adsorption of lead ions (experimental Q_e = 25 mg g^{-1})

Kinetic models	Parameters	Pb(II)
Pseudo-first-order	Q_e (mg g^{-1})	1.88
	k_1 (min^{-1})	0.0083
	R^2	0.974
Pseudo-second-order	Q_e (mg g^{-1})	13.45
	k_2 (g mg^{-1} min^{-1})	0.005
	R^2	0.986

predicted by using these models. Adsorption isotherm was obtained by varying the initial concentration of Pb^{2+} ions from 10–200 mg L^{-1}. As can be seen (Fig. 5a), by increasing the initial concentration the adsorption capacity (Q_e) also increased considerably. The isothermal analysis pointed that the obtained isotherm is following the Type II adsorption pattern as set by IUPAC in 1985 [29].

In this work, the most common adsorption isotherm models namely Langmuir, Freundlich, and Dubinin–Radushkevich models were adopted to examine the collected experimental adsorption data and to evaluate the maximum sorbent uptake capacity (Q_m) for the Pb^{2+} ions.

The Langmuir isotherm model assumes a monolayer adsorption onto the sorbent surface predicting chemisorption tendency having limited homogeneous sites with the adsorption energy conserved and adsorbate transmigration absent. However, Freundlich isotherm is valid for both physisorption (multilayer) and chemisorption (monolayer) adsorption mechanisms. Dubinin–Radushkevich usually confirms the Langmuir isotherm model. Hence, the three mentioned models can be expressed in a linear form according to Eqs. (5)–(8), respectively [30].

$$\frac{C_e}{Q_e} = \frac{C_e}{Q_m} + \frac{1}{K_L Q_m} \tag{5}$$

$$\ln Q_e = \ln K_F + \left(\frac{1}{n}\right) \ln C_e \tag{6}$$

$$\ln Q_e = \ln Q_s + K_{ad}\left(\varepsilon^2\right) \tag{7}$$

$$\varepsilon = RT \ln\left(1 + \frac{1}{C_e}\right) \tag{8}$$

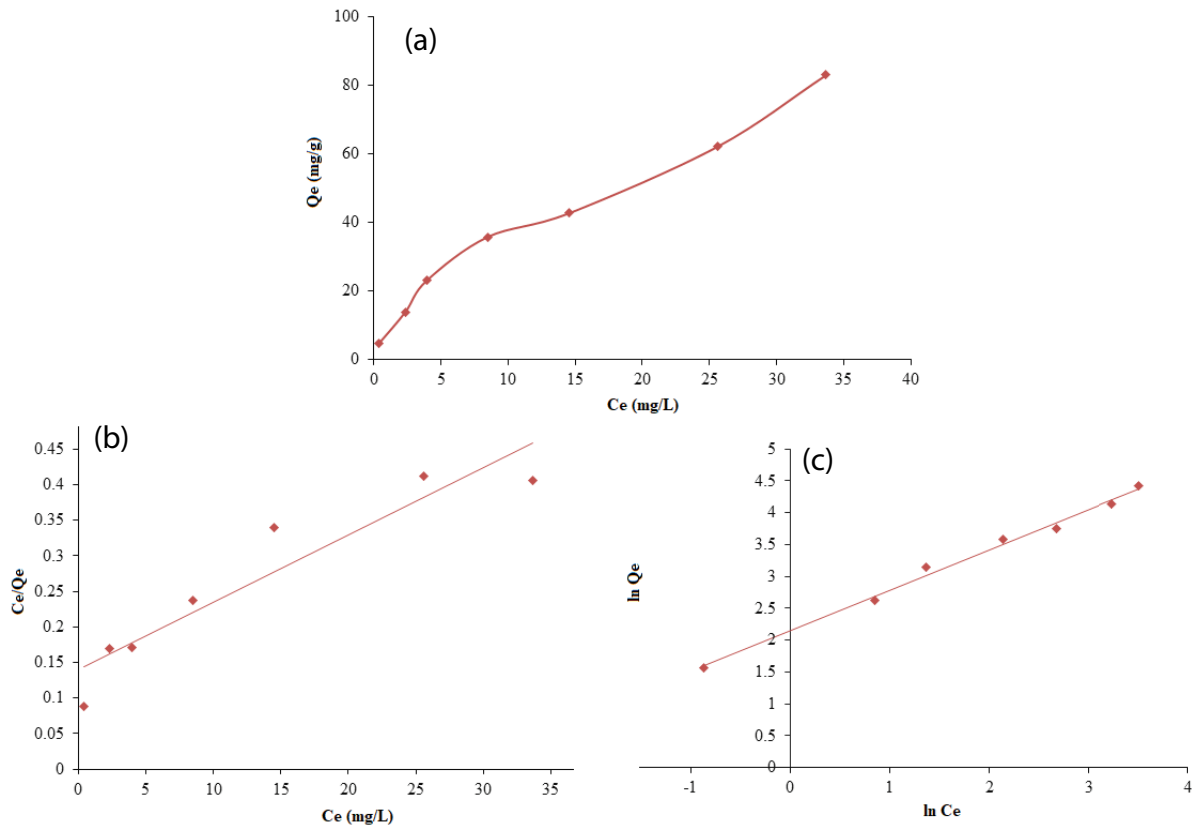$$E = \left(2K_{ad}\right)^{-1/2} \tag{9}$$

Fig. 5. (a) Adsorption equilibrium and isotherm models (b) and (c).

where K_L, K_F, and K_{ad} are equilibrium Langmuir constant (L mg^{-1}), Freundlich constant [(mg g^{-1}) (L mg^{-1})$^{1/n}$], and Dubinin constant related to sorption energy (mol^2 kJ^{-2}), respectively. n is the intensity of adsorption index lying between 1 and 10 showing the strength and favourability of interaction, Q_e and Q_m are the equilibrium and maximum monolayer amount of lead ions adsorbed onto the sorbent (mg g^{-1}), respectively, and C_e the concentration of lead ions remained at equilibrium (mg L^{-1}), Q_s is the theoretical sorption capacity (mg g^{-1}), T (Kelvin) is the temperature, and R is the gas constant (0.008314 kJ mol^{-1} K^{-1}). E is the sorption energy, where, if value of E is <40kJ mol^{-1}, the adsorption pattern follows the physisorption mechanism, whereas if values ranges from 40 to 800 kJ mol^{-1}, it indicates chemisorption pattern [31,32].

The different model parameters of each equation were computed by plotting the graphs (Figs. 5b and c) and the results are summarized in Table 2. Based on the higher value of R^2, it was proposed as which model represents the data better and the obtained results pointed that Freundlich model better fits with the data. Hence, the mechanism of Pb^{2+} ions adsorption onto the Fe$_2$O$_3$-MTMOS was found to be in compliance with the multilayer sorption with no further addition of adsorbate by the physisorption force ($E < 40$ kJ mol^{-1}). The Freundlich constant value (K_F) was found to be lower for sorption process but is still acceptable since sorption capacity generally can explain by adsorption isotherm.

Finally, the freshly prepared Fe$_2$O$_3$-MTMOS sphere were successfully reused for 10 successive adsorption–desorption

Table 2
Isotherm parameters for adsorption of lead ions

Isotherms	Parameters	Pb(II)
	Q_m (mg g^{-1})	105.5
Langmuir	K_L (L mg^{-1})	0.066
	R^2	0.885
	K_F [(mg g^{-1}) (L mg^{-1})$^{1/n}$]	7.35
Freundlich	n	1.57
	R^2	0.993
	Q_s (mg g^{-1})	38.99
Dubinin–Radushkevich	K_{ad} (mol^2 kJ^{-2})	0.0009
	R^2	0.852
Energy	E (kJ/mol)	23.57

cycles for the adsorption of lead(II) ion without any significant decrease in percentage removal. For regeneration, magnetic sphere adsorbent were washed with diluted hydrochloric acid (0.1 N) and distilled water after each cycle of removal.

3.6. Comparison

The lead(II) removal performance of newly fabricated Fe$_2$O$_3$-MTMOS was compared with recently reported adsorbents in terms of pH, contact time, and adsorption capacity and the compared parameter are listed in Table 3.

Table 3
Comparison of adsorption efficiency

Adsorbents	Sample	pH	Time (min)	Q_e (mg g^{-1})	References
Spherical Fe_2O_3-MTMOS	Wastewater	5	150	105.5	This study
Cyclone steel dust	Aqueous solution	5.7	120	39.8	[33]
Sulfonated MNPs	Water	7	10	108.93	[34]
ZnO-montmorillonite	Aqueous solution	4	75	88.5	[35]
N-Fe/OMC	Aqueous solution	3	120	312	[36]
γ-Fe_2O_3/rGO-Ag	Aqueous solution	5	40	90.91	[37]
γ-Fe_2O_3/titanate	Aqueous solution		50	223	[38]
γ-Fe_2O_3	Aqueous solution	5	10	68.9	[39]
Fe_3O_4/PAC	Aqueous solution	6	50	94.3	[40]
Iron-silver	Aqueous solution	3	20	22.88	[41]
AC-Fe_3O_4	Aqueous solution	5	60	57.1	[42]

The magnetic Fe_2O_3-MTMOS adsorbent showed appropriate adsorption capacity (105.5 mg g^{-1}) as compared to cyclone steel dust, sulfonated MNPs, and ZnO-montmorillonite. As evident from the obtained data from Table 3, the prepared Fe_2O_3-MTMOS nanocomposite proposes greater adsorption efficiency for Pb^{2+} ions in a short duration and hence may be employed for effective treatment of heavy metals removal from polluted water thereby addressing the peril of environmental pollution.

4. Conclusion

Spherical magnetic nanocomposite based on methyltrimethoxysilane (Fe_2O_3-MTMOS) was synthesized via sol–gel method and applied for removal of toxic lead ions from wastewater aqueous solution. Three well-known isotherm models were applied for validation of experimental data and Freundlich isotherm model was found to be well-fitted with the obtained results predicting multilayer pattern for lead ions uptake onto Fe_2O_3-MTMOS. By considering the experimental and theoretical values for Q_e, pseudo-second-order kinetic model was well fitted to adsorption process. Moreover, free energy analysis suggested physical adsorption for multilayer adsorption of lead ions on the surface of Fe_2O_3-MTMOS. Hence, the synthesised spherical magnetic Fe_2O_3-MTMOS nanocomposite can be applied as an alternative adsorbent for wastewater treatment.

Acknowledgment

References

[1] M.A. Gabris, B.H. Jume, M. Rezaali, S. Shahabuddin, H. Rashidi Nodeh, R. Saidur, Novel magnetic graphene oxide functionalized cyanopropyl nanocomposite as an adsorbent for the removal of Pb(II) ions from aqueous media: equilibrium and kinetic studies, Environ. Sci. Pollut. Res., 25 (2018) 27122–27132.

[2] P.A. Kobielska, A.J. Howarth, O.K. Farha, S. Nayak, Metal-organic frameworks for heavy metal removal from water, Coord. Chem. Rev., 358 (2018) 92–107.

[3] A. Tayyebi, M. Outokesh, Supercritical synthesis of a magnetite-reduced graphene oxide hybrid with enhanced adsorption properties toward cobalt & strontium ions, RSC Adv., 6 (2016) 13898–13913.

[4] M. Ahmadi, M.H. Niari, B. Kakavandi, Development of maghemite nanoparticles supported on cross-linked chitosan (γ-Fe_2O_3@CS) as a recoverable mesoporous magnetic composite for effective heavy metals removal, J. Mol. Liq., 248 (2017) 184–196.

[5] A. Eslami, R. Nemati, Removal of heavy metal from aqueous environments using bioremediation technology–review, J. Health Field, 3 (2017).

[6] C. Anyakora, Heavy metal contamination of ground water : the surulere case study, Res. J. Environ. Earth Sci., 2 (2010) 39–43.

[7] M.K. Mohammadi Nodeh, M.A. Gabris, H. Rashidi Nodeh, M. Esmaeili Bidhendi, Efficient removal of arsenic(III) from aqueous media using magnetic polyaniline-doped strontium–titanium nanocomposite, Environ. Sci. Pollut. Res., 25 (2018) 16864–16874.

[8] M. Arbabi, S. Hemati, M. Amiri, Removal of lead ions from industrial wastewater: a review of removal methods, Shahrekord Univ. Med. Sci., 2 (2015) 105–109.

[9] S. Shahabuddin, C. Tashakori, M.A. Kamboh, Z. Sotoudehnia Korrani, R. Saidur, H. Rashidi Nodeh, M.E. Bidhendi, Kinetic and equilibrium adsorption of lead from water using magnetic metformin-substituted SBA-15, Environ. Sci. Water Res. Technol., 4 (2018) 549–558.

[10] S.N.A. Baharin, N.M. Sarih, S. Mohamad, S. Shahabuddin, K. Sulaiman, A. Máamor, Removal of endocrine disruptor di-(2-ethylhexyl) phthalate by modified polythiophene-coated magnetic nanoparticles: characterization, adsorption isotherm, kinetic study, thermodynamics, RSC Adv., 6 (2016) 44655–44667.

[11] S. Shahabuddin, N. Muhamad Sarih, S. Mohamad, J. Joon Ching, $SrTiO_3$ nanocube-doped polyaniline nanocomposites with enhanced photocatalytic degradation of methylene blue under visible light, Polymers, 8 (2016) 27.

[12] A. Ahmad, H. Ahmad, D. Lokhat, A. Golandaj, D. Ramjugernath, S.H. Mohd-Setapar, Recent Advances in Polyaniline-Based Nanocomposites as Potential Adsorbents for Trace Metal Ions, In: Polymer-based Nanocomposites for Energy and Environmental Applications, Woodhead Publishing, 2018, pp. 597–615.

[13] Z. Shi, C. Xu, H. Guan, L. Li, L. Fan, Y. Wang, L. Liu, Q. Meng, R. Zhang, Magnetic metal organic frameworks (MOFs) composite for removal of lead and malachite green in wastewater, Colloids Surf., A, 539 (2018) 382–390.

[14] S. Shahabuddina, N.M. Sarih, S. Mohamad, S.N. Atika Baharin, Synthesis and Characterization of Co_3O_4 nanocube doped polyaniline nanocomposites with enhanced methyl

orange adsorption from aqueous solution, RSC Adv., 6 (2016) 43388–43400.

[15] L. Giraldo, A. Erto, J.C. Moreno-Piraján, Magnetite nanoparticles for removal of heavy metals from aqueous solutions: synthesis and characterization, Adsorption, 19 (2013) 465–474.

[16] S. Rajput, C.U. Pittman Jr, D. Mohan, Magnetic magnetite (Fe_3O_4) nanoparticle synthesis and applications for lead (Pb^{2+}) and chromium (Cr^{6+}) removal from water, J. Colloid Interface Sci., 468 (2016) 334–346.

[17] W. Wu, Z. Wu, T. Yu, C. Jiang, W.-S. Kim, Recent progress on magnetic iron oxide nanoparticles: synthesis, surface functional strategies and biomedical applications, Sci. Technol. Adv. Mater., 16 (2015) 23501.

[18] M. Ahmadi, M. Foladivanda, N. Jaafarzadeh, Z. Ramezani, B. Ramavandi, S. Jorfi, B. Kakavandi, Synthesis of chitosan zero-valent iron nanoparticles-supported for cadmium removal: characterization, optimization and modeling approach, J. Water Supply Res. Technol., 66 (2017) 116–130.

[19] W.A. Wan Ibrahim, H.R. Nodeh, H.Y. Aboul-Enein, M.M. Sanagi, Magnetic solid-phase extraction based on modified ferum oxides for enrichment, preconcentration, and isolation of pesticides and selected pollutants, Crit. Rev. Anal. Chem., 45 (2015) 270–287.

[20] M.K. Mohammadi Nodeh, M. Radfard, L.A. Zardari, H. Rashidi Nodeh, Enhanced removal of naproxen from wastewater using silica magnetic nanoparticles decorated onto graphene oxide; parametric and equilibrium study, Sep. Sci. Technol., 15 (2018) 2476–2485.

[21] I.A. Rahman, V. Padavettan, Synthesis of silica nanoparticles by sol–gel: size-dependent properties, surface modification, and applications in silica-polymer nanocomposites—a review, J. Nanomater., 2012 (2012) 1–8.

[22] R.M. Amir, F.M. Anjum, M.I. Khan, M.R. Khan, I. Pasha, M. Nadeem, Application of Fourier transform infrared (FTIR) spectroscopy for the identification of wheat varieties, J. Food Sci. Technol., 50 (2013) 1018–1023.

[23] A. Azari, H. Gharibi, B. Kakavandi, G. Ghanizadeh, A. Javid, A.H. Mahvi, K. Sharafi, T. Khosravia, Magnetic adsorption separation process: an alternative method of mercury extracting from aqueous solution using modified chitosan coated Fe_3O_4 nanocomposites, J. Chem. Technol. Biotechnol., 92 (2017) 188–200.

[24] M. Ahmadi, H. Rahmani, B. Ramavandi, B. Kakavandi, Removal of nitrate from aqueous solution using activated carbon modified with Fenton reagents, Desal. Water Treat., 76 (2017) 265–275.

[25] J. Hu, G. Chen, I.M.C. Lo, Selective removal of heavy metals from industrial wastewater using maghemite nanoparticle: performance and mechanisms, J. Environ. Eng., 132 (2006) 709–715.

[26] F. Jamali-Behnam, A.A. Najafpoor, M. Davoudi, T. Rohani-Bastami, H. Alidadi, H. Esmaily, M. Dolatabadi, Adsorptive removal of arsenic from aqueous solutions using magnetite nanoparticles and silica-coated magnetite nanoparticles, Environ. Prog. Sustainable Energy, 37 (2018) 951–960.

[27] S. Abbaszadeh, S.R. Wan Alwi, N. Ghasemi, H. Rashidi Nodeh, C. Colin Webb, I.I. Muhamad, Use of pristine papaya peel to remove Pb(II) from aqueous solution, Chem. Eng. Trans., 45 (2015) 961–966.

[28] K.S. Padmavathy, G. Madhu, P.V. Haseena, A study on effects of pH, adsorbent dosage, time, initial concentration and adsorption isotherm study for the removal of hexavalent chromium (Cr(VI)) from wastewater by magnetite nanoparticles, Procedia Technol., 24 (2016) 585–594.

[29] K.S.W. Sing, Reporting physisorption data for gas/solid systems with special reference to the determination of surface area and porosity (IUPAC recommendations 1984), Pure Appl. Chem., 57 (1985) 603–619.

[30] M. Massoudinejad, A. Asadi, M. Vosoughi, M. Gholami, M.A. Karami, A comprehensive study (kinetic, thermodynamic and equilibrium) of arsenic(V) adsorption using $KMnO_4$ modified clinoptilolite, Korean J. Chem. Eng., 32 (2015) 2078–2086.

[31] T.A. Saleh, Isotherm, kinetic, and thermodynamic studies on Hg(II) adsorption from aqueous solution by silica-multiwall carbon nanotubes, Environ. Sci. Pollut. Res., 22 (2015) 16721–16731.

[32] S. Mona, A. Kaushik, Chromium and cobalt sequestration using exopolysaccharides produced by freshwater cyanobacterium *Nostoc linckia*, Ecol. Eng., 82 (2015) 121–125.

[33] Z.B. Bouabidi, M.H. El-Naas, D. Cortes, G. McKay, Steel-making dust as a potential adsorbent for the removal of lead(II) from an aqueous solution, Chem. Eng. J., 334 (2018) 837–844.

[34] K. Chen, J. He, Y. Li, X. Cai, K. Zhang, T. Liu, Y. Hu, D. Lin, L. Kong, J. Liu, Removal of cadmium and lead ions from water by sulfonated magnetic nanoparticle adsorbents, J. Colloid Interface Sci., 494 (2017) 307–316.

[35] H.A. Sani, M.B. Ahmad, M.Z. Hussein, N.A. Ibrahim, A. Musa, T.A. Saleh, Nanocomposite of ZnO with montmorillonite for removal of lead and copper ions from aqueous solutions, Process Saf. Environ. Prot., 109 (2017) 97–105.

[36] Y. Zhou, X. Liu, L. Tang, F. Zhang, G. Zeng, X. Peng, L. Luo, Y. Deng, Y. Pang, J. Zhang, Insight into highly efficient co-removal of p-nitrophenol and lead by nitrogen-functionalized magnetic ordered mesoporous carbon: performance and modelling, J. Hazard. Mater., 333 (2017) 80–87.

[37] B.N. Haerizade, M. Ghavami, M. Koohi, S. Janitabar Darzi, N. Rezaee, M.Z. Kassaee, Green removal of toxic Pb(II) from water by a novel and recyclable Ag/γ-Fe_2O_3@r-GO nano-composite, Iran. J. Chem. Chem. Eng., 37 (2018) 1–10.

[38] H. Chen, T. Li, L. Zhang, R. Wang, F. Jiang, J. Chen, Pb(II) adsorption on magnetic γ-Fe_2O_3/titanate nanotubes composite, J. Environ. Chem. Eng., 3 (2015) 2022–2030.

[39] S. Rajput, L.P. Singh, C.U. Pittman Jr, D. Mohan, Lead (Pb^{2+}) and copper (Cu^{2+}) remediation from water using superparamagnetic maghemite (γ-Fe_2O_3) nanoparticles synthesized by flame spray pyrolysis (FSP), J. Colloid Interface Sci., 492 (2017) 176–190.

[40] B. Kakavandi, A. Jonidi Jafari, R. Rezaei Kalantary, S. Nasseri, A. Esrafili, A. Gholizadeh, A. Azari, Simultaneous adsorption of lead and aniline onto magnetically recoverable carbon: optimization, modeling and mechanism, J. Chem. Technol. Biotechnol., 91 (2016) 3000–3010.

[41] A. Azari, R.R. Kalantary, G. Ghanizadeh, B. Kakavandi, M. Farzadkia, E. Ahmadi, Iron–silver oxide nanoadsorbent synthesized by co-precipitation process for fluoride removal from aqueous solution and its adsorption mechanism, RSC Adv., 5 (2015) 87377–87391.

[42] R. Rezaei Kalantary, E. Dehghanifard, A. Mohseni-Bandpi, L. Rezaei, A. Esrafili, B. Kakavandi, A. Azari, Nitrate adsorption by synthetic activated carbon magnetic nanoparticles: kinetics, isotherms and thermodynamic studies, Desal. Water Treat., 57 (2016) 16445–16455.